Research Article

Modified Crossed-Wire Antennas Radiating a Circularly Polarized Conical Beam

Kazuhide Hirose [iD],[1] **Kazuhiko Hata,**[1] **and Hisamatsu Nakano**[2]

[1]*College of Engineering, Shibaura Institute of Technology, Tokyo 135-8548, Japan*
[2]*Science and Engineering, Hosei University, Tokyo 184-8584, Japan*

Correspondence should be addressed to Kazuhide Hirose; khirose@sic.shibaura-it.ac.jp

Two types of modified crossed-wire antennas are investigated to enhance a circularly polarized (CP) wave bandwidth. The wire length of each antenna is increased twice as long as that of the original antenna. First, a bent-type antenna is analyzed using the method of moments. It is found that the CP wave bandwidth for a 3 dB axial ratio criterion is twice as wide as that of the original antenna. Next, a spiral-type antenna is analyzed. It is revealed that the antenna shows a CP wave bandwidth of 28%, which is wider than that of the original antenna by a factor of 3.5. The analysis results are validated by experimental work.

1. Introduction

Mobile satellite communications have often required an antenna radiating a circularly polarized (CP) conical beam [1]. For this requirement, many antennas have been investigated [2–5]. These antennas are mainly divided into two classes: planar [2, 3] and nonplanar [4, 5]. In addition, there have been three kinds of radiators used in the nonplanar antennas; they are an aperture [5], slot [6], and monopole [4].

A crossed-wire antenna shown in Figure 1(a)is in a class with the nonplanar antennas having a monopole radiator [7]. The antenna has an advantage over a conventional one [2–6] in that the maximum radiation can be obtained at a lower elevation-angle direction. So far, there has been no investigation to increase the CP wave bandwidth.

The purpose of this paper is to increase the CP wave bandwidth of a crossed-wire antenna. For this, two types of antennas with increased wire length are analyzed using the method of moments [8]; one is a bent-type antenna shown in Figure 1(b) and the other is a spiral-type antenna shown in Figure 1(e), each having wire o–o' shown Figure 1(c) as a monopole radiator. The radiation characteristics including the axial ratio, beam direction, input impedance, and

radiation pattern are discussed and compared with those of the original antenna [7] shown in Figure 1(d).

2. Bent-Type Antenna

In this section, the arm length of the original antenna [7] shown in Figure 1(d) is increased. The effects of the increased arm length on the radiation characteristics are investigated.

Figures 1(a)–1(c) illustrate a bent-type antenna, which is made of wires of radius ρ. Four bent arms symmetrical with respect to the cross point o' are backed by a ground plane at height h. The arms are fed at the cross point o' through a vertical wire o'-o of length h, as shown in Figure 1(c), and the bottom end o is excited by a coaxial line. To obtain CP radiation, four parasitic elements of length h and radius ρ are added symmetrically with respect to the cross point o' [7]. The location (x, y) of the parasitic element is designated as (d_x, d_y), as shown in Figure 1(b). Note that the bottom end of each parasitic element is short-circuited to the ground plane.

The antenna is designed to radiate a CP wave in the maximum beam direction. For this, the parasitic element location (d_x, d_y) is appropriately selected [7] using the method of moments [8]. To enhance the CP wave
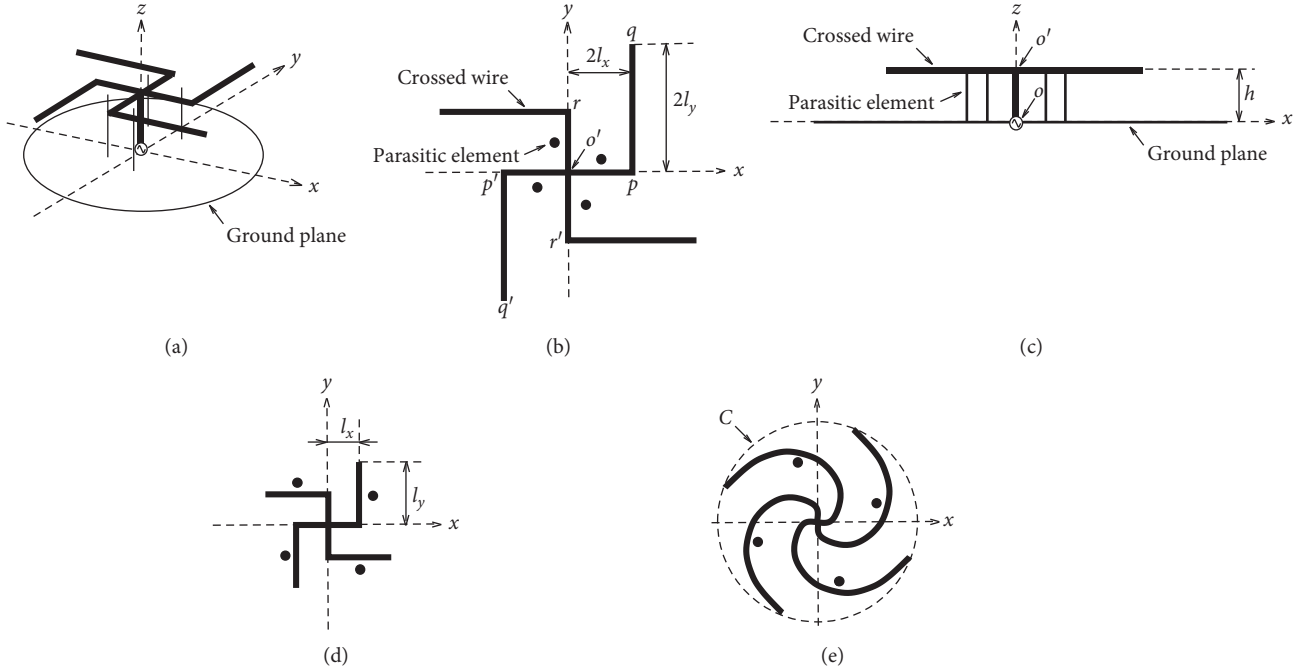
FIGURE 1: Antenna configurations. (a) Perspective view. (b) Top view of bent-type antenna. (c) Side view. (d) Original antenna [7]. (e) Spiral-type antenna.

bandwidth, the bent arm length is taken to be twice $(2l_x + 2l_y)$ as long as that $(l_x + l_y = 3\lambda_0/8)$ of the original antenna, as shown in Figures 1(b) and 1(d), where l_x and l_y are element lengths in the x and y directions of the bent arm in the first quadrant, respectively, and λ_0 is the free-space wavelength at a test frequency of f_0. The other configuration parameters are chosen to be the same as those of the original antenna [7]: $(h, \rho, l_x, l_y) = (\lambda_0/4, \lambda_0/85, \lambda_0/8, \lambda_0/4)$. Note that the ground plane is assumed to be of an infinite extent and image theory is used in the analysis [7].

A numerical result of the axial ratio versus frequency for $(d_x, d_y) = (2\lambda_0/32, 4\lambda_0/32)$ is shown with a solid line in Figure 2(a). The axial ratio is evaluated in the maximum beam direction. It is found that the antenna has a CP wave bandwidth of 15% for a 3 dB axial ratio criterion. For comparison, a dotted line shows the result of the original antenna, which has a bandwidth of 8% [7]. The bandwidth of the bent-type antenna is twice as wide as that of the original antenna. A solid line of Figure 2(b) shows the beam direction θ versus frequency, where the direction remains almost unchanged (at $\theta = 53° \pm 2.5°$) in the CP wave bandwidth.

The input impedance as a function of frequency is shown with solid lines in Figure 2(c). It is observed that the real part of the impedance R_{in} reaches $1300\,\Omega$ at a lower frequency in the CP wave bandwidth.

Finally, we explain why the antenna can radiate a CP wave when the parasitic element location (d_x, d_y) is selected. For simplicity, we consider radiation components of E_θ and E_ϕ in the $\phi = 0°$ plane. Referring to the antenna coordinate system shown in Figure 1, we see that partial radiation from the parasitic elements has only the E_θ component. On the other hand, partial radiation from both the four bent arms and vertical wire o'-o has not only the E_θ component but also

the E_ϕ component since each arm is bent. To be more specific, the E_ϕ component occurs from wires p-q and p'-q' in the bent arms shown in Figure 1(b), since partial radiation from the wire o'-r cancels out that from the wire o'-r' due to their current distributions having the same amplitudes with a phase difference of 180° (this implies a fact that if the four arms were straight, the antenna could not radiate a CP wave even when the parasitic element location is selected). The selection of (d_x, d_y) leads to the E_θ component appropriate for CP radiation. It can be said that appropriate radiation of the E_θ component by the selection of (d_x, d_y) enables the antenna to radiate a CP wave.

The abovementioned explanation suggests a method for increasing the CP wave bandwidth. Since the selection of (d_x, d_y) contributes to the control of the E_θ component, it is necessary to control the E_ϕ component. We can control the E_ϕ component by increasing the arm length and/or by changing the arm shape. From this point of view, we first increase the arm length in this section and then change the bent arms into spiral ones in the next section.

3. Spiral-Type Antenna

So far, we have investigated the effects of an increased arm length on the radiation characteristics of a bent-type antenna. In this section, a bent arm with an increased length is further transformed into a spiral one shown in Figure 1(e). The effects of the spiral arm on the radiation characteristics are investigated.

Figure 3 shows a spiral-type antenna of circumference C, where the arms are symmetrical with respect to the cross point o'. Each arm #n ($n = 1, 2, 3,$ and 4) is defined by an equiangular spiral function with a spiral constant a_s and an
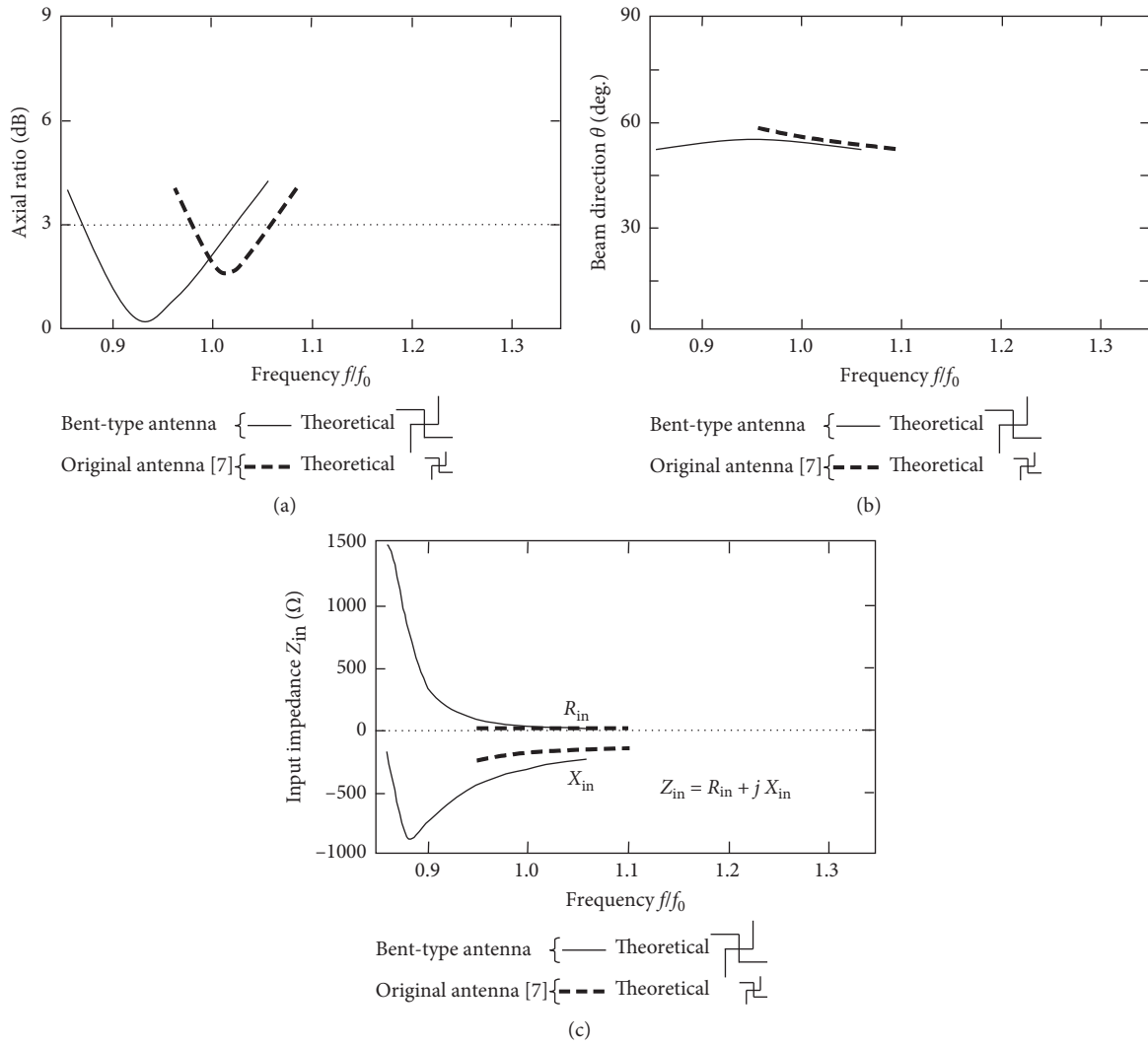
FIGURE 2: Frequency responses of axial ratio, beam direction, and input impedance of bent-type antenna for $(d_x, d_y) = (2\lambda_0/32, 4\lambda_0/32)$, together with those of the original antenna [7]. (a) Axial ratio. (b) Beam direction. (c) Input impedance.
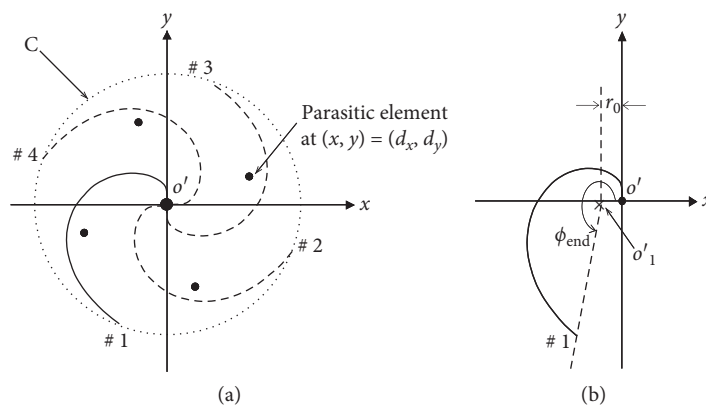

FIGURE 3: Spiral-type antenna. (a) Arms #n ($n = 1, 2, 3,$ and 4) with cross point o'. (b) Spiral origin o'_n. Arm shape is defined by the equiangular spiral function: $r = r_0 \cdot \exp[a_s \cdot \{\phi_s - (n-1) \cdot \pi/2\}]$, where r is the radial distance from the spiral origin o'_n to a point on the spiral arm #n, r_0 is the initial length of r, a_s is a spiral constant, and ϕ_s is a winding angle ranging $(n-1) \cdot \pi/2 \leq \phi_s \leq (n-1) \cdot \pi/2 + \phi_{end}$ with ϕ_{end} being the end winding angle.
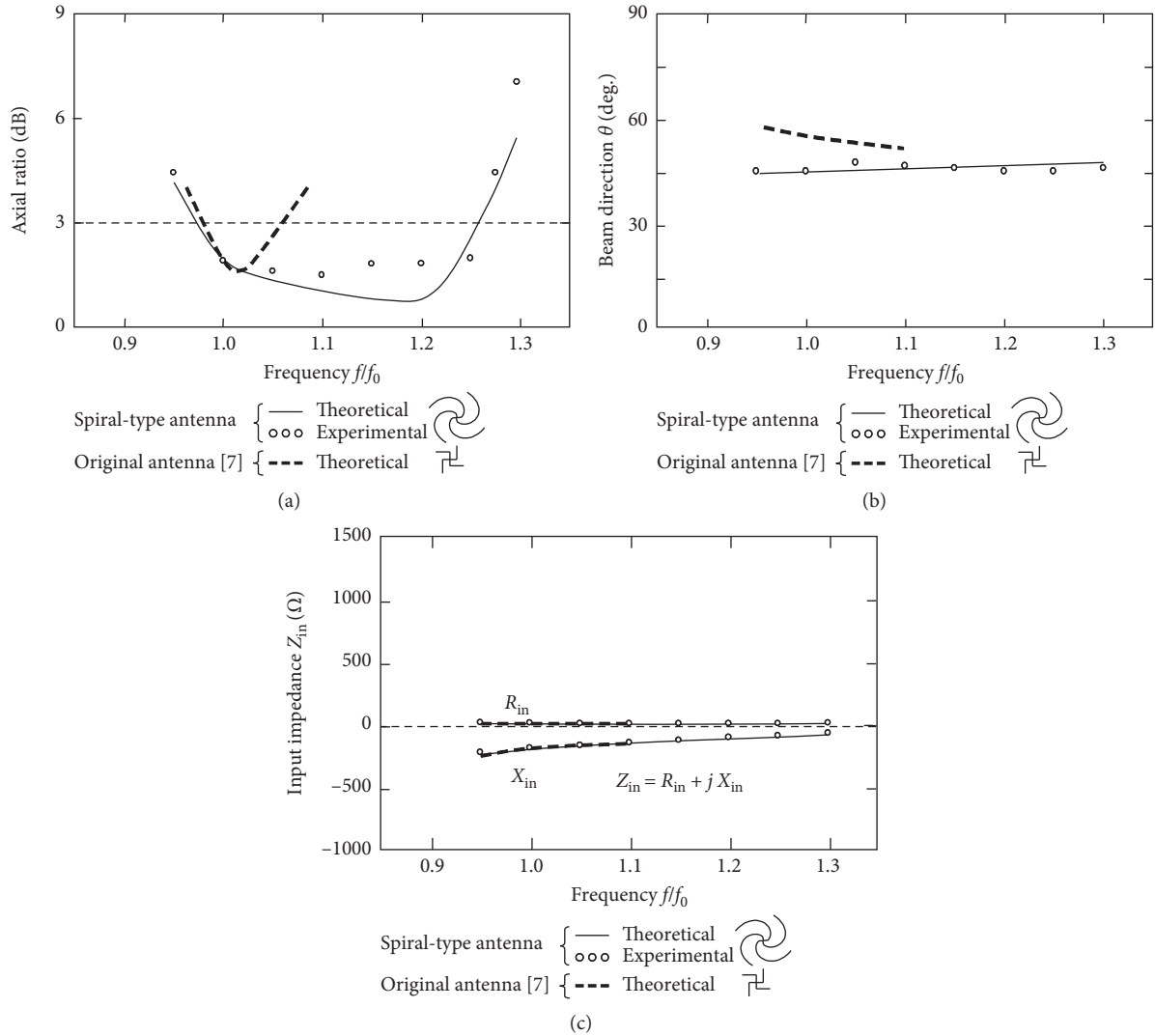
FIGURE 4: Frequency responses of axial ratio, beam direction, and input impedance of a spiral-type antenna for $(d_x, d_y) = (57\lambda_0/256, 15\lambda_0/256)$, together with those of the original antenna [7]. (a) Axial ratio. (b) Beam direction. (c) Input impedance.

end winding angle ϕ_{end}. Note that the spiral origin o'_n is shifted from the cross point o' by a distance of r_0, as shown in Figure 3(b).

The antenna circumference is chosen to be a typical value ($C = 2.4\lambda_0$) for a conventional spiral antenna to radiate a CP conical beam [9]. The arm length is taken to be the same as that ($3\lambda_0/4$) in section 2. From these two values, the two spiral parameters are determined to be $(a_s, \phi_{end}) = (0.5 \text{ rad}^{-1}, 4.5 \text{ rad})$ for a distance of $r_0 = 0.04\lambda_0$. The other configuration parameters are the same as those in section 2, except for the parasitic element location (d_x, d_y).

The location (d_x, d_y) is again optimized for CP radiation. The numerical result of the axial ratio versus frequency for $(d_x, d_y) = (57\lambda_0/256, 15\lambda_0/256)$ is shown with a solid line in Figure 4(a), together with that of the original antenna. It is emphasized that the antenna shows a CP wave bandwidth of 28%, which is wider than that of the original antenna by a factor of 3.5.

A solid line in Figure 4(b) shows the frequency response of the maximum beam direction. It is observed that the

direction is almost constant ($\theta = 46° \pm 1°$) in the CP wave bandwidth. In fact, the slight variation is half that of ($\pm 2.5°$) the bent-type antenna in section 2. It can be said that the spiral arm contributes to not only enhancement in the CP wave bandwidth but also to stabilization of the beam direction.

Stabilization in the input impedance versus frequency is also obtained. This is shown with solid lines in Figure 4(c). It is found that the real part of the impedance remains almost unchanged at $R_{in} = 14 \, \Omega$ in the CP wave bandwidth (while the R_{in} of the bent-type antenna reaches $1300 \, \Omega$ in section 2). Note that the input impedance of the original antenna is also shown with dotted lines, which are not visible as they overlap the solid lines.

Figures 5(a) and 5(b) show typical radiation patterns in the $\phi = 0°$ and $45°$ planes, respectively, for $(d_x, d_y) = (57\lambda_0/256, 15\lambda_0/256)$. The pattern in the $\phi = 90°$ plane is the same as that in the $\phi = 0°$ plane due to the symmetrical antenna configuration with respect to the coordinate origin, o. Solid and dotted lines show the numerical results of left-hand (E_L)
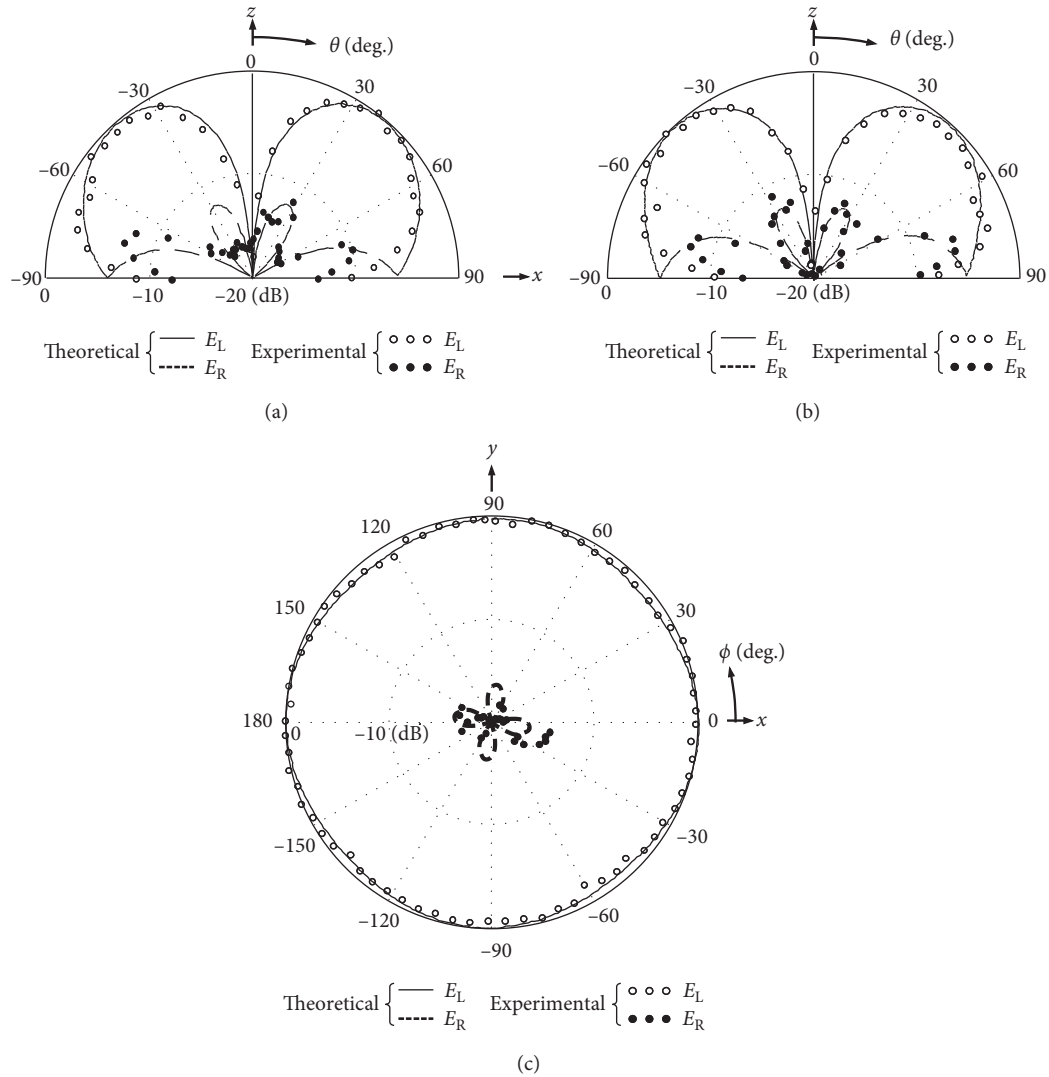
(a)

(b)

(c)

FIGURE 5: Radiation patterns of spiral-type antenna for $(d_x, d_y) = (57\lambda_0/256, 15\lambda_0/256)$ at $f = 1.0f_0$. (a) $\phi = 0°$ plane, where the beam direction is $\theta = 46°$. (b) $\phi = 45°$ plane. (c) $\theta = 46°$ plane.

and right-hand (E_R) CP wave components, respectively. It is observed that the antenna radiates a CP conical beam. The maximum beam directions are $\theta = 46°$ and $44°$ in the $\phi = 0°$ and $45°$ planes, respectively. Angle coverages where the axial ratio is less than 3 dB are $20°$ and $18°$ in the $\phi = 0°$ and $45°$ planes, respectively. The gain is approximately 5 dB.

Solid and dotted lines in Figure 5(c) show the numerical result of the radiation pattern in the $\theta = 46°$ plane, where the maximum radiation is obtained. It is found that the principal polarization component E_L remains almost unchanged versus angle ϕ. The variation in E_L is within 0.8 dB.

4. Experimental Work

In this section, the numerical results in section 3 are validated by experimental work. For this, we fabricate a spiral-type antenna using the ground plane of $12\lambda_0 \times 12\lambda_0$ at $f_0 = 7$ GHz. Pictures of the fabricated antenna are shown in Figure 6. The radiation patterns are measured in an anechoic chamber using a horn antenna (Narda 642) at a distance of 3 m from the test antenna. The test antenna is rotated on a turntable, while the horn antenna is fixed. The input impedance is measured using a network analyzer (HP 8719C).

Small circles in Figure 4 show the experimental results of the frequency responses of the axial ratio, beam direction, and input impedance. They agree well with the numerical results shown with solid lines.

Agreement between the experimental and numerical results is also obtained for the radiation patterns shown in Figure 5. Small circles and dots show the experimental results of principal (E_L) and cross polarization (E_R) components, respectively. The corresponding numerical results are shown with solid and dotted lines.

Before concluding the investigation of modified crossed-wire antennas, we compare the results with those of existing nonplanar antennas. The comparison is summarized in Table 1. It is emphasized that the spiral-type antenna (prototype) has a wider CP wave bandwidth than the other
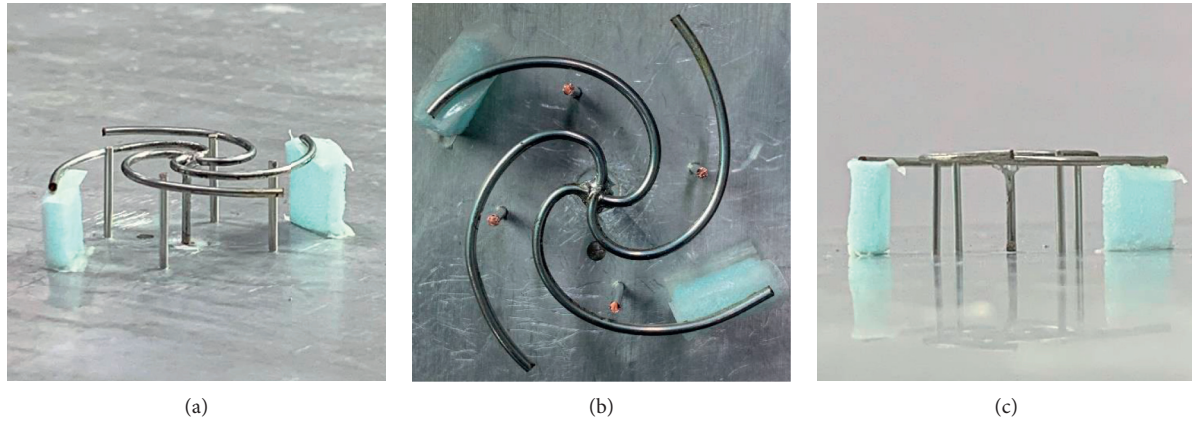
FIGURE 6: Pictures of the prototype used in the experimental work. (a) Perspective view. (b) Top view. (c) Side view.

TABLE 1: Comparison with other nonplanar antennas.

Radiator in antenna	CP wave bandwidth (%)	Profile ($x \times y \times$ height)	Beam direction from zenith (°)
Aperture [5]	5	$1.6\lambda \times 1.6\lambda \times 1.0\lambda$	28
Slot [6]	9	$2.5\lambda \times 2.5\lambda \times 1.0\lambda$	45
Monopole [4]	22	$1.0\lambda \times 1.0\lambda \times 0.35\lambda$	35
Monopole [7]	8	$0.50\lambda \times 0.50\lambda \times 0.25\lambda$	55
Monopole [10]	3*	$0.48\lambda \times 0.48\lambda \times 0.45\lambda$	50
Monopole (prototype)	28	$0.76\lambda \times 0.76\lambda \times 0.25\lambda$	46

*3% is the bandwidth for VSWR < 1.5.

antennas. In addition, the prototype with increased arm length still has a small antenna size and a large-angle beam direction from the zenith (a low elevation-angle direction) in comparison with the other antennas.

5. Conclusions

Using the method of moments, we have investigated a crossed-wire antenna modified for wideband circularly polarized (CP) radiation. First, the bent arm length of the original antenna is increased. It is found that the CP wave bandwidth becomes twice that of the original antenna. Subsequently, the bent arm with an increased length is transformed into a spiral one. It is demonstrated both numerically and experimentally that the antenna shows a CP wave bandwidth of 28%, which is 3.5 times as wide as that of the original antenna.

Input impedance matching a 50 ohm coaxial line has yet to be researched.

Data Availability

The numerical and experimental data used to support the findings of this study are included within the article.

Conflicts of Interest

The authors declare that there are no conflicts of interest regarding the publication of this paper.

References

[1] J. R. James and P. S. Hall, *Handbook of Microstrip Antennas*, Peregrinus, Stevenage, U.K, 1989.

[2] H. Xu, J. Zhou, Q. Wu, Z. Yu, and W. Hong, "Wideband low-profile SIW cavity-backed circularly polarized antenna with high-gain and conical-beam radiation," *IEEE Transactions on Antennas and Propagation*, vol. 66, no. 3, pp. 1179–1188, 2018.

[3] W. Lin and H. Wong, "Circularly polarized conical-beam antenna with wide bandwidth and low profile," *IEEE Transactions on Antennas and Propagation*, vol. 62, no. 12, pp. 5974–5982, 2014.

[4] S. Karki, M. Sabbadini, K. Alkhalifeh, and C. Craeye, "Metallic monopole parasitic antenna with circularly polarized conical patterns," *IEEE Transactions on Antennas and Propagation*, vol. 67, no. 8, pp. 5243–5252, 2019.

[5] S.-S. Qi, W. Wu, and D.-G. Fang, "Singly-fed circularly polarized circular aperture antenna with conical beam," *IEEE Transactions on Antennas and Propagation*, vol. 61, no. 6, pp. 3345–3349, 2013.

[6] G. Chenhu, J. Geng, H. Zhou et al., "Truncated circular cone slot antenna array that radiates a circularly polarized conical beam," *IEEE Antennas and Wireless Propagation Letters*, vol. 16, pp. 2574–2577, 2017.

[7] K. Hirose and T. Wada, "A bent, crossed wire antenna with vertical parasitic elements:formation of a circularly polarized

conical beam," *IEICE Transactions,* vol. J84-B, no. 9, pp. 1164–1672, 2001.

[8] R. F. Harrington, *Fields Computation by Moment Methods*, Macmillan, New York, NY, USA, 1968.

[9] K. Hirose, H. Sato, and H. Nakano, "Spiral antennas radiating a circularly polarized conical beam," in *Proceedings of IEEE Antennas and Propagation Society International Symposium*, pp. 602–605, Washington, DC, USA, 2005.

[10] H. Kawakami, G. Sato, and R. Wakabayashi, "Research on circularly polarized conical-beam antennas," *IEEE Antennas and Propagation Magazine*, vol. 39, no. 3, pp. 27–39, 1997.